Conformational Behavior of Macromolecules in Solution. Homopolypeptides of α-Aminoisobutyric Acid as Test Cases

Roberto Improta, Nadia Rega, Carlos Aleman,† and Vincenzo Barone*

Dipartimento di Chimica, Università di Napoli Federico II, Complesso Universitario Monte S. Angelo, Via Cintia, I-80126, Napoli, Italy

Received April 13, 2001; Revised Manuscript Received June 29, 2001

ABSTRACT: Solvent effects on the conformational preferences of homopolypeptides constituted by α-aminoisobutyric acid (polyAib) have been investigated coupling the polarizable continuum model (PCM) either to a quantum mechanical (PBE0/6-31G(d)) or to a molecular−mechanical (Amber) representation of the solute. The results allow a deeper insight into the influence of the solvent on the 3_{10}/α-helix equilibrium in polyAib and show that PCM/Amber is a useful tool to study the conformational preferences of large peptides in condensed phase. As a matter of fact, all the PCM/Amber results are close to their PCM/PBE0 counterparts, except for some underestimation of the absolute solvation energies in polar solvents.

1. Introduction

Although α-aminoisobutyric acid (Aib) is not one of the 20 "standard" amino acids, in the last two decades many experimental and theoretical papers have been devoted to the study of Aib-rich oligopeptides.[1−10] Aib indeed widely occurs in vivo in microbial peptides (as the peptaibol) which play a key role in causing voltage-dependent conductance in membranes.[11] There is a general agreement on the fact that the presence of Aib in membrane-spanning peptides is related to its conformational preferences: the presence of two methyl substituents at the C^{α} strongly favors the formation of helix (either α or 3_{10}) secondary structures. As a matter of fact, due to its peculiar structural features, Aib has been widely used in synthetically designed macromolecules as a helix-inducing peptide; the great amount of interest in trying to understand Aib conformational preferences is thus explained also by its relevance for protein engineering. It has been shown that the equilibrium between the α- and 3_{10}-helix in Aib-containing oligopeptides is strongly influenced by subtle changes in several parameters, such as the peptide length, the relative number of Aib residues, and the solvent polarity.[1,2,4a,12]

In a previous quantum mechanical study, we have indeed shown that the 3_{10}-helix is the preferred conformation for an infinite Aib homopolymer (hereafter AibIH) in vacuo,[13] in agreement with IR evidence for Aib polymers in the solid state.[12] However, this result holds for an infinite polypeptide in vacuo, whereas, as we have seen, there are at least two additional effects that can play a fundamental role in determining the preferred conformation of Aib-containing polypeptides, i.e., the number of residues and the polarity of the solvent. The study of these two latter factors is tackled in the present paper, where we report an analysis of the relative stability of α- and 3_{10}-helices for Aib homopolypeptides, varying the number of residues (from 1 to 15) and the nature of the embedding medium (from gas phase to aqueous solution).

An analysis of the factors influencing the equilibrium between α- and 3_{10}-helices is interesting also because it has been suggested that the 3_{10} structure is an important intermediate in protein folding;[14−18] furthermore a $3_{10} \rightarrow \alpha$ helix transition can be a crucial step in some enzymatic reactions.[19]

Solvent effects are taken into account by means of the polarizable continuum model (PCM).[20,21] The quantum mechanical (QM) implementation of this method has indeed allowed the prediction of solvation energies close to the so-called "chemical accuracy" and provides both accurate values of spectroscopic parameters and reliable descriptions of static and dynamic phenomena in condensed phase.[22−26]

In this paper PCM calculations are coupled both to QM and to molecular mechanics (MM) representations of the solute. QM computations have been performed in the framework of density functional theory (DFT), since a high accuracy is required when dealing with conformational equilibria of polypeptides often governed by very subtle effects. Unfortunately, the computational cost of correlated methods has until now restricted their use to the study of medium-size molecules, but for very recent studies of isolated molecules.[27,28]

In the present paper we show that the recent improvements of PCM implementation allow QM calculations in condensed phase for solutes containing a few hundred atoms. Nevertheless, due the very large size of the macromolecules of biological interest, the coupling of the PCM with a MM representation of the solute remains an important target. Following previous partial attempts,[29] we have recently completed a very effective PCM/MM implementation allowing the evaluation of solvation free energies and of their analytical gradients.[30,31] Since this implementation has been included in the Gaussian series of programs,[32] it can benefit from all our recent improvements for the treatment of large systems[33−36] and can use all the force fields already present in this package (Dreiding,[37] UFF,[38] and Am-

† Permanent address: Departament d'Enginyeria Química, Universitat Politècnica de Catalunya, E.T.S. d'Enginyers Industrials de Barcelona, Diagonal 647, Barcelona E-08028, Spain.

* Corresponding author. E-mail: enzo@lsdm.dichi.unina.it.

10.1021/ma0106503 CCC: $20.00
Published on Web 09/15/2001

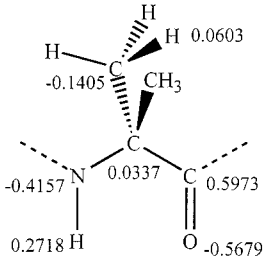

Figure 1. Molecular structure and atomic charges of the Aib residue.

ber[39]). Here we have used the Amber force field, which was specifically parametrized for the study of biological systems. Thus, together with its intrinsic interest the present study has allowed also the assessment of the suitability of the PCM/Amber procedure to describe solvent effects on the conformational preferences of large molecules of biological interest.

Concerning the choice of the solvent to consider in PCM calculations, we selected chloroform and water. Chloroform (in which Aib polypeptides are soluble) can be taken as a general model of low-polarity solvents. On the other hand, even if Aib oligopeptides are hardly soluble in water, the study of this solvent can give useful insights into the influence of an increase of the solvent polarity on the equilibrium between 3_{10}- and α-helices, since this effect should be significantly enhanced in water.

2. Methods

All the calculations were carried out with a development version of the Gaussian package.[32]

DFT calculations have been performed at the PBE0 level[40] and using the 6-31G(d) basis set.[41] The PBE0 model is a parameter-free hybrid Hartree−Fock/DFT method rooted in the adiabatic connection formula[42] and based on fourth-order perturbation theory:[40]

$$E_{xc}^{PBE0} = E_{xc}^{PBE} + \frac{1}{4}(E_{xc}^{HF} - E_{x}^{PBE}) \quad (1)$$

where E_x^{HF} is the Hartree−Fock exchange and E_x^{PBE} and E_{xc}^{PBE} are the exchange and the complete density functional proposed by Perdew, Burke, and Ernzerhof (PBE), respectively.[43] The PBE functional is particularly attractive, since it is based on a number of limiting conditions and does not involve empirical parameters.[43] Its remarkable reliability is further increased including some HF exchange (eq 1), especially in the field of conformational studies of biomolecules.[44]

MM computations have been performed by the implementation of Amber[39] available in the Gaussian package. MM geometry optimizations have been performed by using analytical gradients and the standard algorithms[45] implemented in the Gaussian package. In the gas-phase calculations fast equation solving methods[45b] particularly suitable for handling large size systems have been exploited. The atomic charges used for the Aib residue (see Figure 1) were determined at the HF/6-31G(d) level and are compatible with the second generation of the Amber force field.[39]

Atomic charges for the Ace and NMe end groups were directly transferred from Amber libraries.[39]

Solvent effects have been taken into account by the PCM. In this method the solvent is represented by an infinite dielectric medium characterized by the relative dielectric constant of the bulk (4.90 for $CHCl_3$ and 78.39 for H_2O). A molecular-shaped surface contains the system under study (the solute) and separates it from the surrounding solvent. The cavity including the molecule, defined in terms of interlocking spheres centered on non-hydrogen atoms, is built by the GePol procedure[47] using the UAHF atomic radii.[46] The free energy of solvation (ΔG_{solv}) includes electrostatic, dispersion/repulsion, and cavitation contributions:

$$\Delta G_{solv} = \Delta G_{el} + \Delta G_{dr} + \Delta G_{cav}$$

The cavitation term is determined using the Pierotti's scaled particle theory,[48] while ΔG_{dr} is evaluated using semiempirical atom−atom parameters.[49] Finally ΔG_{el} takes into account the solute−solvent electrostatic interaction: in the quantum mechanical implementation this contribution is obtained adding a proper operator to the solute Hamiltonian. If $\hat{H}^{vac}$ is the solute Hamiltonian in the gas phase and Ψ^{vac} and Ψ^{sol} are the solute wave functions optimized in the gas phase and in solution, respectively, the electrostatic contribution to ΔG_{sol} is

$$\Delta G_{el} = \langle \Psi^{sol} | \hat{H}^{vac} | \Psi^{sol} \rangle - \langle \Psi^{vac} | \hat{H}^{vac} | \Psi^{vac} \rangle - \frac{1}{2}\sum_i q_i V_i \quad (2)$$

where the sum on right-hand side runs on the finite elements (tesserae) covering the cavity surface.[47] V is the solute electrostatic potential; the q_i's are the apparent charges representing the solvent reaction field: they are calculated on the basis of classic electrostatics equations and depend on the solute electron density. Thus, the difference between the first and the second term on the right-hand side of eq 2 is the solvation energy due to the molecule polarization by the solvent, while the last sum represents the electrostatic solute−solvent interaction. The molecular mechanics implementation of the method does not consider the solute polarization by the solvent, so that the ΔG_{el} reduces to

$$\Delta G_{el} = -\frac{1}{2}\sum_i q_i V_i$$

where both V and q's are calculated from suitable atomic charges.

In this work we have used the CPCM[21b] variant of PCM, which, employing conductor rather than dielectric boundary conditions, allows a more robust implementation. Analytical energy first and second derivatives of eq 2 allow for geometry optimizations and harmonic frequency calculations in solution at both the QM and MM levels.[21c]

Note that all the terms of the solvation energy can be dissected into contributions issuing from the different spheres forming the cavity. Since each sphere corresponds to a well-defined atom (or chemical group), this procedure allows a detailed analysis of the origin of differential solvation effects. However, the electrostatic contribution of each sphere originates from the electron density of the whole solute, so that this analysis should be considered only qualitative.

The solvation energy per residue has been calculated subtracting from the total value of the solvation energy the contribution of the *N*-methylacetamide molecule (which is formed by joining both polypeptide cappings) and then dividing by the number of residues. Although different choices would have been possible, the relative solvation energy per residue of the two helices remains unchanged.

3. Results and Discussion

The chemical structure of the Aib residue is displayed in Figure 1. The homopolypeptides studied were Ac−$(Aib)_n$−NMe (hereafter denoted Aib_n), where Ac is acetyl, NMe is *N*-methyl, and *n* is the number of Aib residues. Since our main interest is to determine the influence of the solvent on the energy of "ideal" polyAib helices, in DFT calculations the geometry of Aib residues has been kept frozen to that optimized for the infinite homopolypeptide in vacuo by DFT calculations employing periodic boundary conditions (PBC)[13] (see Table 1

Table 1. Selected Geometrical Parameters (bond lengths in Å and angles in deg) of Helical Structures of Aib Obtained by PBC Computations[a]

	3_{10}	α
ϕ	−51.3 (−54)[b]	−55.4 (≈−55)[c]
ψ	−25.3 (−28)[b]	−43.8 (≈−45)[c]
ω	177.5 (176.1)[d]	175.6
CN	1.357 (1.34)[d]	1.362
CO	1.230 (1.23)[d]	1.247
$C^{\alpha}-N$	1.472 (1.47)[d]	1.473
$C^{\alpha}-C$	1.559 (1.54)[d]	1.558
$N-C^{\alpha}-C$	111.4 (111.1)[d]	109.9

[a] Experimental average values are given in parentheses. [b] Ref 47. [c] Ref 5a. [d] Ref 10.

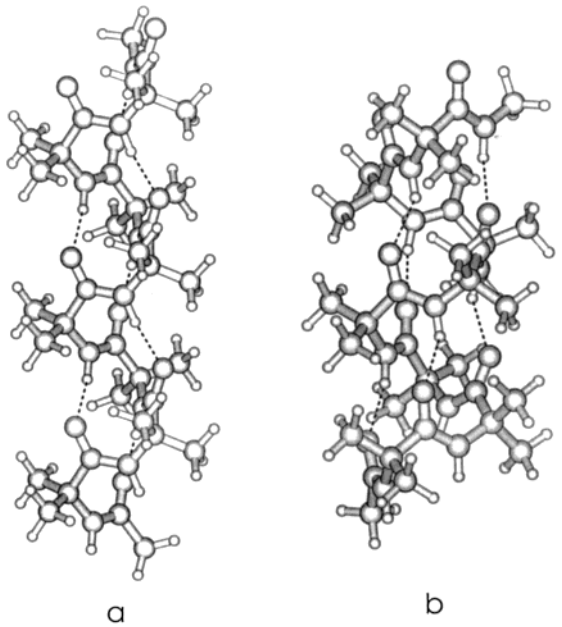

Figure 2. 3_{10}-helix (a) and α-helix (b) structures of $(Aib)_8$, as optimized for the Aib infinite homopolypeptide by PBC computations at the PBE/6-31G(d) level.

and Figure 2). Furthermore, here and in the following we will make reference to left-handed helices, so that ϕ and ψ have negative values.

It is worth noting that the geometry used for the 3_{10}-helix is in good agreement with the X-ray structure of the Aib decapeptide.[4a] Moreover the calculated values of ϕ and ψ dihedral angles (−51.3° and −25.3°, respectively) agree with the average found for Aib residues in the 3_{10}-helix ($\phi = -54°$, $\psi = -28°$).[50] In AibIH the geometry of the α-helix is strongly distorted (vide infra); however, the average values of ϕ and ψ ($\phi = -55.4°$, $\psi = -43.8°$) are close to the experimental averages ($\phi \approx -55°$, $\psi \approx -45°$, according to ref 5a or $\phi \approx -57°$, $\psi \approx -50°$ according to ref 11) of Aib α-helices in polypeptides.

3.1. Aib Dipeptide Analogue $(Aib)_1$. Let us first analyze the behavior of $(Aib)_1$, i.e., the dipeptide analogue of the Aib residue. The study of this compound can give useful insights into the interplay of local components of intrinsic and environmental effects in determining the equilibrium between 3_{10}- and α-helices, and it is thus relevant for evaluating the contribution of a single Aib residue to the conformation of a generic polypeptide chain.

Inspection of Table 2 shows that an increase of the polarity of the embedding medium favors the α-helix over the 3_{10}-helix: the 3_{10}-helix is indeed more stable

Table 2. Most Relevant Results of the PCM Calcualtions on $(Aib)_1$

	3_{10} helix			α-helix		
	gas phase	$CHCl_3$	H_2O	gas phase	$CHCl_3$	H_2O
	PBE0					
ϕ	−51.3	−51.3	−51.3	−55.4	−55.4	−55.4
ψ	−25.3	−25.3	−25.3	−43.8	−43.8	−43.8
ΔG_{sol}	0	−4.97	−13.43	0	−5.56	−14.18
ΔG_{el}	0	−6.98	−17.45	0	−7.63	−18.31
$\Delta G_{non\ electr}$[a]	0	2.01	4.02	0	2.07	4.13
total exp. surf.[b]	227.92	227.92	227.92	228	228	228
polar exp. surf.[c]	53.8	53.8	53.8	54.7	54.7	54.7
dipole moment[d]	5.97	7.28	8.53	6.44	7.89	9.27
	Amber					
ϕ	−51.3	−51.3	−51.3	−55.4	−55.4	−55.4
ψ	−25.3	−25.3	−25.3	−43.8	−43.8	−43.8
ΔG_{sol}	0	−5.78	−10.62	0	−6.6	−11.67
ΔG_{el}	0	−7.8	−14.64	0	−8.67	−15.81
$\Delta G_{non\ electr}$[a]	0	2.02	4.02	0	2.07	4.13
total exp. surf.[b]	227.92	227.92	227.92	228.1	228.1	228.1
dipole moment[d]	7.44	7.44	7.44	8.07	8.07	8.07

[a] $\Delta G_{non\ electr} = \Delta G_{dr} + \Delta G_{cav}$. [b] Total surface exposed to the solvent. [c] Sum of the surface exposed to the solvent by the spheres associated with oxygen atoms and NH groups. [d] In debye.

Table 3. Most Relevant Results of the PCM Geometry Optimizations of the Aib Dipeptide Analogue

	PBE0/6-31G(d)			Amber		
	vacuum	$CHCl_3$	H_2O	vacuum	$CHCl_3$	H_2O
ϕ	−66.8	−62.7	−58.3	C7	−52.7	−50.2
ψ	−25.2	−33.2	−37.3		12.6	−20.8
ΔG_{sol}	0	−4.32	−11.96		−3.50	−9.98
ΔG_{el}	0	−6.14	−15.69		−5.24	−13.77
$\Delta G_{non\ electr}$[a]	0	1.82	3.73		1.74	3.79
total exp. surf.[b]	226.2	225.6	225.5		226.37	227.14
polar exp. surf.[c]	53.7	53.4	53.3		52.44	52.04
dipole moment[d]	5.53	7.14	8.74		4.39	7.01

[a] $\Delta G_{non\ electr} = \Delta G_{dr} + \Delta G_{cav}$. [b] Total surface exposed to the solvent. [c] Sum of the surface exposed to the solvent by the spheres associated with oxygen atoms and with NH groups. [d] In debye.

in vacuo (by 0.5 kcal/mol), whereas in $CHCl_3$ and, even more, in water the α-helix is slightly more stable.

The increasing stabilization of the α-helix with the solvent polarity is probably due to the concurrence of different effects. The dipole moment of the α-helix is larger than that of the 3_{10}-helix (9.27 vs 8.53 D for $(Aib)_1$) in aqueous solution. Furthermore, although the total surface exposed to the solvent is very similar in both helices, the most polar atoms (oxygen and nitrogen) are better exposed to the solvent in the α-helix (vide infra). Finally, in the α-helix there is a more favorable arrangement of positive (NH) and negative (O) moieties, which allows the maximization of the interaction with the solvent. PCM/PBE0/6-31G(d) geometry optimizations confirm this picture: the minimum energy helix geometry is 3_{10}-like in vacuo, intermediate between the 3_{10}- and α-helix in $CHCl_3$, and α-like in water (see Table 3).

PCM/Amber calculations give quite similar results from a qualitative point of view: the α-helix is stabilized by an increase of solvent polarity. However the 3_{10}-helix remains more stable also in aqueous solution, due to the excessive stabilization of the 3_{10}-helix predicted by the Amber force field in vacuo (1.4 kcal/mol at the Amber level and 0.5 kcal/mol at the PBE0 level). As a matter of fact, PCM/Amber calculations predict that the relative stabilization of the α-helix in aqueous solution is even larger than that predicted at the PCM/PBE0/

Table 4. Solvation Free Energies (kcal/mol) Obtained by PCM/PBE0/6-31G(d) and PCM/Amber Computations for the α-Helix Relative to the 3_{10}-Helix of Homopolypeptides of Aib[a]

	PBE0/6-31G(d)			Amber		
	gas phase[b]	$CHCl_3$	H_2O	gas phase[b]	$CHCl_3$	H_2O
$(Aib)_1$	0.51	−0.59 (−0.59)	−0.75 (−0.75)	1.42	−0.82 (−0.82)	−1.05 (−1.05)
$(Aib)_2$	2.85	−1.38 (−0.69)	−2.76 (−1.39)	3.53	−2.94 (−1.40)	−4.29 (−2.14)
$(Aib)_3$	3.48	−2.54 (−0.85)	−3.26 (−1.08)	8.68	−4.13 (−1.37)	−5.53 (−1.85)
$(Aib)_4$	5.28	−4.86 (−1.22)	−6.54 (−1.63)	13.47	−6.05 (−1.51)	−8.21 (−2.05)
$(Aib)_5$	6.23	−7.31 (−1.46)	−10.17 (−2.03)	16.23	−8.14 (−1.62)	−10.94 (−2.19)
$(Aib)_6$	6.81	−9.34 (−1.56)	−12.79 (−2.13)	17.99	−9.63 (−1.61)	−13.01 (−2.16)
$(Aib)_7$	7.17	−10.64 (−1.52)	−15.06 (−2.15)	19.22	−10.88 (−1.56)	−14.66 (−2.10)
$(Aib)_8$	7.41	−12.05 (−1.50)	−17.05 (−2.13)	20.12	−12.05 (−1.51)	−15.98 (−1.99)

[a] Values per residue are given in parentheses. [b] Relative energy per residue.

6-31G(d) level. Actually, the Amber force field seems to underestimate the stabilization of helices, which do not correspond to relative minima on the potential energy surface of the dipeptide analogue in vacuo. PCM/Amber geometry optimizations starting from 3_{10}-/α-helix geometries fall, indeed, in the C7 conformation in vacuo and in a conformation intermediate between C7 and 3_{10}-helix in $CHCl_3$. Only in aqueous solution does the 3_{10}-helix become a relative minimum of the potential energy surface.

A detailed comparison of the PCM/Amber and PCM/PBE0 implementations indicates that the Amber version (i) yields good estimates of the relative stability of different helical structures; (ii) provides quite accurate (albeit slightly overestimated) solvation energies in $CHCl_3$; and (iii) underestimates the electrostatic contribution with respect to PCM/PBE0/6-31G(d) in aqueous solution. These are very reasonable results, since the polarization of the solute is not taken into account in PCM/Amber calculations. Thus, the work needed to perturb the solute charge distribution in the gas phase to the solvent-adapted values is neglected in the PCM/Amber method, which uses a fixed set of charges to describe the solute. The charges used in MM calculations are slightly too large with respect to their QM values in vacuo or in apolar solvents, but, being nonpolarizable, they are too small for calculations in aqueous solution and this leads to some underestimation of the electrostatic contribution to the hydration energy (see dipoles collected in Table 2).

3.2. $(Aib)_n$ Homopolypeptides. We have then compared the values of ΔG_{sol} obtained from PCM/PBE0/6-31G(d) and PCM/Amber methods for the α- and 3_{10}-helices of Aib_n homopeptides (see Table 4 and Figure 3).

Helical geometries were obtained according to the procedure discussed in section 2. Confirming the trend found at the dipeptide level, the α-helix is always favored by the increase of solvent polarity (see Figure 3). As already evidenced in the preceding paragraph, in the α-helix polar groups (mainly oxygen atoms) are better exposed to the solvent (see Figure 4).

Since it exhibits an *i*/*i*+3 hydrogen bonding pattern, the 3_{10}-helix can form one intrachain hydrogen bond more than the α-helix, which has an *i*/*i*+4 hydrogen bond pattern (see Figure 2). This effect obviously favors the 3_{10}-helix, whose relative stability with respect to the α-helix increases in vacuo by ∼5.2 kcal/mol when going from Aib_1 to Aib_2: this is just the order of magnitude expected for the presence of an additional hydrogen bond in the 3_{10}-helix. However, the same effect contributes to the greater solvent stabilization of the α-helix, which has an amido group not engaged in a hydrogen bond and, thus, is better exposed to the solvent. PCM

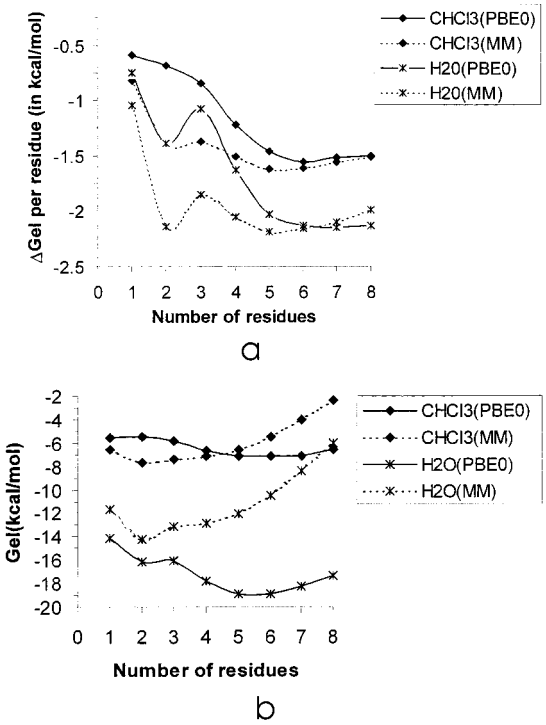

Figure 3. (a) Free energies of solvation (kcal/mol) per residue of the α-helix relative to the 3_{10}-helix obtained for Aib homopolypeptides using the PCM/PBE0/6-31G(d) (solid lines) and PCM/Amber (dashed lines) methods in $CHCl_3$ and in water. (b) Total free energies of solvation (kcal/mol) of the α-helix obtained for Aib homopolypeptides using the PCM/PBE0/6-31G(d) (solid lines) and PCM/Amber (dashed lines).

allows evaluating the order of magnitude of this effect, since it is possible to determine the contribution of the sphere associated with each atom or group to the total G_{el}.

It is important to recall that this value depends on the simultaneous interactions among all the solvation charges and the solute electron density and, thus, can be considered a local property only to a first approximation. It is, however, noteworthy that in $(Aib)_2$ the sum of the contributions of the (NH) and (CO) groups involved in the intramolecular H-bond in the 3_{10}-helix decreases in this conformation by ∼2 kcal/mol with respect to the α-helix. This value is a significant percentage of the total difference between the solvation energy of the 3_{10}- and α-helix, which is 2.76 kcal/mol.

The relative effect on the solvation energy of the presence of an additional hydrogen bond in the 3_{10}-helix is expected to decrease with the increase of the peptide length. However PBE0/6-31G(d) calculations predict that the difference between the solvation energy per

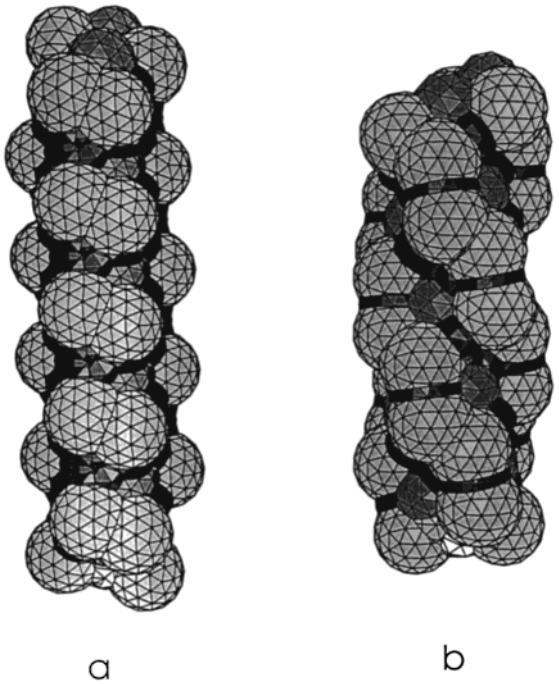

Figure 4. Gepol cavities for 3_{10}-helix (a) and α-helix (b) structures of $(Aib)_{15}$. White, light gray, and dark gray tesserae belong to the spheres embedding amidic groups, methyl groups, and oxygen atoms, respectively. The spheres added to smooth the molecular surface[44] are depicted in black.

residue of the 3_{10}- and α-helix continues to increase up to 7 residues.

This result is probably due to the fact that, as shown in ref 13, in the α-helix the residues are arranged in the ideal way to maximize dipole−dipole interactions. This effect can thus stabilize, cooperatively, more dipolar electronic structures in each residue. As a matter of fact, net charges of oxygen atoms become more negative when going toward the C-terminus of the homopolypeptides. As a consequence, the contribution to the solvation energy of the spheres associated with a C-terminal carbonyl moiety increases with the peptide length, although the solvent-exposed surface is the same irrespective of the number of repeating units (see Figure 5). A similar trend is found for the NH group, even if, of course, the solvation energy of this group increases going toward the N-terminus.

These effects are present also in the 3_{10} helix, but, due to the smaller stabilization coming from dipole−dipole interactions,[13] they are less important. This explains why the difference between the solvation energy of the two helices does not reach a plateau for 7 residues. On the other hand, the α-helix has a repeating unit of ∼7 residues, and it is thus likely that after 7or 8 residues the C-terminal carbonyl moiety will experience the same dipolar interactions and, consequently, will have a similar interaction with the solvent, irrespective of the peptide length.

PCM/Amber calculations provide a similar picture: the α-helix is more favored than the 3_{10}-helix by solvent effects, both in $CHCl_3$ and in water, with a similar dependence on the peptide length. The relative stabilization of the α-helix seems to be slightly overestimated in water up to $n = 4/5$; for $n > 5$ ab initio and MM values are more similar. This result is probably due to some error compensation in Amber calculations, which neglect charge polarization effects due to dipole−dipole interactions (vide infra).

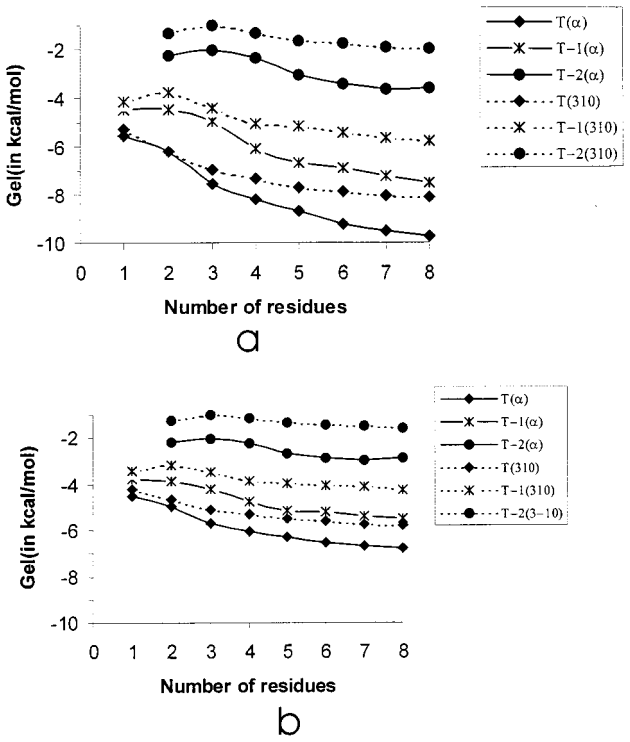

Figure 5. Contribution to the total electrostatic solvation energy of the spheres associated with the three last C-terminal oxygen atoms (labeled T, T-1, and T-2, respectively) of Aib in the α-helix (solid lines) and in the 3_{10}-helix (dashed lines) calculated using (a) PCM/PBE0/6-31G(d) and (b) PCM/Amber.

Table 5. Solvation Free Energies (kcal/mol) Obtained by PCM/6-31G(d) and PCM/Amber for the 3_{10}- and the α-Helix $(Aib)_n$ ($n = 1-8$)

	PBE0/631G(d)				Amber			
	$CHCl_3$		H_2O		$CHCl_3$		H_2O	
$(Aib)_n$	3_{10}	α	3_{10}	α	3_{10}	α	3_{10}	α
$(Aib)_1$	−4.97	−5.56	−13.43	−14.18	−5.78	−6.6	−10.62	−11.67
$(Aib)_2$	−4.07	−5.45	−13.42	−16.18	−4.9	−7.69	−9.92	−14.21
$(Aib)_3$	−3.28	−5.82	−12.84	−16.1	−3.25	−7.38	−7.63	−13.16
$(Aib)_4$	−1.77	−6.63	−11.3	−17.84	−1.04	−7.09	−4.66	−12.87
$(Aib)_5$	0.18	−7.13	−8.73	−18.9	1.53	−6.61	−1.07	−12.01
$(Aib)_6$	2.22	−7.12	−6.13	−18.92	4.14	−5.49	2.48	−10.53
$(Aib)_7$	4.05	−6.59	−3.17	−18.23	6.87	−4.01	6.3	−8.36
$(Aib)_8$	7.05	−5.00	−0.28	−17.33	9.73	−2.32	9.94	−6.04

Confirming the feature sketched above, PCM/Amber underestimates the total solvation energy in water (see Table 5).

The absence of charge polarization in this method decreases the importance of cooperative interactions: the charge assigned to each atom is always the same, irrespective of its position in the polypeptide. However, the contribution of the C-terminus oxygen sphere to the solvation energy is predicted to decrease with the polypeptide length also at the Amber level (see Figure 5), although the slope of the curve is smaller than that predicted at the PCM/PBE0 level. This confirms that the contribution of each sphere to the solvation energy is not an entirely local property. The smaller weight of dipole−dipole interactions in Amber calculations leads to more similar solvation energies for both helices: the differential solvent stabilization per residue reaches indeed its maximum value already for $n = 5$.

Despite the larger solvent stabilization of the α-helix, inspection of Table 4 shows that the 3_{10}-helix is favored over the α-helix for the $(Aib)_n$ series, irrespective of the

Table 6. Backbone Dihedral Angles (deg) and Free Energies (kcal/mol) Obtained by Amber (gas phase) and Amber/PCM (aqueous solution) Optimizations of $(Aib)_{15}$ Helices

	Amber		Amber/PCM	
	3_{10}-helix	α-helix	3_{10}-helix	α-helix
φ	−45.50	−49.35	−46.13	−49.49
ψ	−29.12	−58.45	−27.85	−58.70
ΔG_{el}	−32.26	−42.05	−33.88	−46.33
ΔG_{nel}[a]	68.95	81.40	69.07	81.33
G_{vac}[b]	−21.84	−9.83	−20.88	−6.72
G_{tot}[c]	14.85	29.52	14.24	28.28

[a] $\Delta G_{nel} = \Delta G_{dr} + \Delta G_{cav}$. [b] G_{vac} = free energy in vacuo. [c] $G_{tot} = G_{vac} + \Delta G_{sol}$.

polarity of the embedding medium, according to both PCM/PBE0 and PCM/Amber calculations. Moreover, the difference between the 3_{10}- and α-helix increases with the polypeptide length. This result is due to the destabilization of the ideal α-helix for Aib homopolymers, probably due to the presence of a repulsive contact between pairs of methyl substituents at i and i+4 residues, whose distance is less than 3 Å. These unfavorable contacts can be relieved by distorting the α-helix structure toward a geometry intermediate between the α- and 3_{10}-helix (as predicted by PBC calculations) or characterized by "nonstandard" values of the backbone ϕ,ψ dihedrals (see results of MM geometry optimizations).

PCM calculations, both at DFT and at MM levels, predict that, lengthening the polypeptide chain, the importance of non-electrostatic solvation contributions increases at the expense of electrostatic ones. The presence of two methyl substituents at C^{α} makes indeed vanishing the contribution to G_{el} of the "central" residues of the chain. Inspection of Figure 4 shows indeed that solvent-exposed surface of the oxygen atoms in the middle of the chain is very small, mainly for the 3_{10}-helix.

On the other hand, the sum of non-electrostatic contributions to the solvation energy is positive and increases regularly with the number of residues, mainly due to the cavitation energy. This term is larger for the less compact 3_{10}-helix (see Figures 2 and 4), and this factor contributes also to the smaller solvent stabilization of this structure.

3.3. Amber Geometry Optimizations. Table 6 collects the most important geometric parameters of $(Aib)_{15}$ issuing from Amber geometry optimizations both in vacuo and in aqueous solution.

The geometries of the five central residues are practically identical, suggesting that the results of calculations on $(Aib)_{15}$ can be meaningfully compared with those of PBC/DFT calculations.

Both helices correspond to stable minima in vacuo and in solution. However their backbone geometry is quite far from the "standard" experimental structures, mostly for the α-helix. Gas-phase Amber calculations predict average values of $\phi \approx -44°$, $\psi \approx -29°$ in the 3_{10}-helix and $\phi \approx -50°$, $\psi \approx -58°$ in the α-helix. The inclusion of solvent effects by means of the PCM leaves the equilibrium geometries practically unchanged, even if the 3_{10}-helix assumes a geometry ($\phi \approx -46°$,$\psi \approx -28°$) more similar to that predicted by experiments and by PBC calculations.

From the energetic point of view, the 3_{10}-helix is predicted to be more stable than the α-helix both in vacuo and in aqueous solution (by ≈1 kcal/mol and ≈ 0.9 kcal/mol per residue, respectively). It is important to highlight that the solvation energy of the optimized helices does not differ significantly from that of the PBC-like structures; actually the latter ones have a slightly larger solvent stabilization.

4. Discussion and Conclusions

Solvent effects on the conformational preferences of Aib homopolypeptides have been investigated using PCM/PBE0/6-31G(d) and PCM/Amber computational models.

Solvent is confirmed to be a critical factor in determining the conformational preferences of a single Aib residue. PCM calculations (both at the MM and at the DFT level) predict that the 3_{10}-helix is the most stable conformation in vacuo for the Aib dipeptide analogue, whereas in aqueous solution the equilibrium is switched toward the α-helix. The structure is, of course, intermediate in nonpolar solvents, where the two helices are almost isoenergetic. This result is confirmed by PCM/PBE0/6-31G(d) geometry optimizations: the structure of the helix minimum conformation changes from 3_{10}-like to α-like when increasing solvent polarity. Incidentally, our results confirm the helix-inducing power of Aib: at variance with standard amino acids[51] helical structures correspond to local minima of the potential energy surface for the dipeptide analogue already in vacuo. The intrinsic contribution of a single Aib residue to the conformational behavior of a polypeptide chain appears thus to be strongly influenced by the polarity of the embedding medium. This picture changes remarkably in the presence of polyAib stretches. In this case, 3_{10}-helix conformation allows the minimization of methyl−methyl repulsions, at variance with an ideal α-helix. Solvent stabilization cannot overcome this unfavorable interaction, and the 3_{10}-helix is predicted to be more stable than the α-helix even in aqueous solution. Our computational results are in good agreement with experimental findings: Aib homopolypeptides always exhibit 3_{10}-helix conformation, and this structure is progressively favored when the Aib content of a given polypeptide increases. However, the above picture can be modified if α-helix structure is distorted in order to minimize methyl−methyl repulsion. As a matter of fact, PBC geometry optimizations of infinite Aib homopolypeptide predict that in vacuo the 3_{10} helix is more stable than the α-helix by just 0.5 kcal/mol per residue. It cannot be excluded that in solution the 3_{10}-helix is in equilibrium with a distorted α-helix, as suggested by recent experiments on homopolypeptides of another $C^{\alpha,\alpha}$-disubstituted residue.[52] PCM/Amber geometry optimizations show that the equilibrium geometry is not remarkably affected by the solvent, confirming that the use of PBC geometries in PCM/PBE0 calculations should not invalidate the reliability of our conclusions about the influence of solvent effects on 3_{10}-/α-helix equilibrium.

From a methodological point of view, the present paper shows that sophisticated ab initio calculations in condensed phase are nowadays fully feasible also for species containing hundreds of atoms. At the same time, our results indicate that PCM/Amber is an inexpensive model able to provide a quite reliable picture of solvent effects on the conformational preferences of large molecules of biological interest. Thus, the classical description of the solute charge distribution has a potential as a very fast procedure for the computation of free

energies of solvation. This change from a quantum mechanical description of the solute to a classical one simplifies the method, but without a significant decrease in the accuracy of the $\Delta\Delta G_{sol}$ values. However, this strategy results in a systematic underestimation of the electrostatic contribution to the absolute free energy of solvation in water, since polarization effects cannot be accounted for due to the use of fixed atomic charges. Other sources of such underestimation can be found in the charge distribution. The assumption that the molecular charge density can be well represented by atom-centered monopoles has been criticized for complex molecules such as amides.[53] Furthermore, the flexible nature of the peptides investigated adds the changes in charges due to conformational flexibility as a source of error. However, the relative free energies of solvation of the 3_{10}- and α-helix predicted by PCM/Amber are in good agreement with those obtained with sophisticated ab initio methods, except for a small underestimation when the number of residues is between 4 and 7, so that long-range dipole−dipole interactions are more effective. Furthermore, for apolar solvents such as $CHCl_3$ PCM/Amber and PCM/PBE0 solvation energies are very similar also from a quantitative point of view.

In conclusion, we think that, together with their intrinsic interest, the results of the present study pave the route for a reliable and effective representation of solvent effects on the conformational behavior of large molecules of biological interest.

Acknowledgment. The authors thank the Italian Research Council (CNR) and Gaussian Inc. for financial support. C.A. thanks the Universitat Politecnica de Catalunya for financial support when in Napoli.

References and Notes

(1) Wang, Y.; Kuczera, K. *J. Phys. Chem. B* **1997**, *101*, 5205.
(2) Smythe, M. L.; Huston, S. E.; Marshall, M. L. *J. Am. Chem. Soc.* **1995**, *117*, 5445.
(3) (a) Su, G.; Kitao, A.; Hirata, F.; Go, N. *J. Am. Chem. Soc.* **1994**, *116*, 6307. (b) Aleman, C. *J. Phys. Chem. B* **1997**, *101*, 5046.
(4) (a) Toniolo, C.; Crisma, M.; Bonora, G. M.; Benedetti, E.; Di Blasio, B.; Pavone, V.; Pedone, C.; Santini, A. *Biopolymers* **1991**, *31*, 129. (b) Benedetti, E.; Bavoso, A.; Di Blasio, B.; Pavone, V.; Pedone, C.; Crisma, M.; Bonora, G. M.; Toniolo, C. *J. Am. Chem. Soc.* **1982**, *104*, 2437. (c) Toniolo, C.; Crisma, M. *Biopolymers* **1992**, *32*, 453.
(5) (a) Karle, I. L.; Balaram, P. *Biochemistry* **1990**, *29*, 6747. (b) Karle, I. L.; Das, C.; Balaram, P. *Proc. Natl. Acad. Sci. U.S.A.* **2000**, *97*, 3034.
(6) Di Blasio, B.; Pavone, V.; Lombardi, A.; Pedone, C.; Benedetti, E.; Subirana, J. A.; Pérez, J. J. *Biopolymers* **1992**, *32*, 621.
(7) Vijayumar, E. K. S.; Balaram, P. *Tetrahedron* **1983**, *39*, 2725.
(8) Zhang, L.; Hermans, J. *J. Am. Chem. Soc.* **1994**, *116*, 11915.
(9) (a) Alemán, C. *Proteins: Struct, Funct., Genet.* **1997**, *29*, 575. (b) Alemán, C. *J. Phys. Chem. B* **1997**, *101*, 5046. (c) Alemán, C.; Roca, R.; Luque, F. J.; Orozco, M. *Proteins: Struct., Funct., Genet.* **1997**, *28*, 83.
(10) Paterson, Y.; Rumsey, S. M.; Benedetti, E.; Némethy, G.; Scheraga, H. A. *J. Am. Chem. Soc.* **1981**, *103*, 2947.
(11) (a) Marshall, G. D.; Beunsen, D. D. In *Biomembrane Electrochemistry*; Blank, M., Vodyanoy, I., Eds; Advances in Chemistry Series 235; American Chemical Society: Washington, DC, 1994; p 259. (b) Pandey, R. C.; Meng, H.; Cook, J. C.; Rinehart, K. L. *J. Am. Chem. Soc.* **1977**, *99*, 5203.
(12) (a) Malcom, B. R. *Biopolymers* **1977**, *16*, 2591. (b) Malcom, B. R. *Biopolymers* **1982**, *22*, 319. (c) Krimm, S.; Owivedi, A. M. *Proc. I.U.P.A.C. Macromol. Symp.* 28th, **1982**, 41.
(13) Improta, R.; Barone, V.; Kudin, K.; Scuseria, G. E. *J. Am. Chem. Soc.* **2001**, *123*, 3311.
(14) Tirado-Rives, J.; Maxwell, D. S.; Jorgensen, W. L. *J. Am. Chem. Soc.* **1993**, *115*, 11590.
(15) Takano, M.; Yamato, T.; Higo, J.; Suyama, A.; Nakayama, K. *J. Am. Chem. Soc.* **1999**, *121*, 605.
(16) Bertsch, R. A.; Vaidehi, N.; Chan, S. I.; Goddard, W. A., III. *Proteins* **1998**, *33*, 343.
(17) Tobias, D. J.; Brooks, C. L. *Biochemistry* **1991**, *30*, 6059.
(18) (a) Bolin, K. A.; Millhauser, G. L. *Acc. Chem. Res.* **1999**, *32*, 1027. (b) Millhauser, G. L. *Biochemistry* **1995**, *34*, 3873.
(19) (a) Gerstein, M.; Chothia, C. *J. Mol. Biol.* **1991**, *220*, 133. (b) McPalen, C. A.; Vincent, M. G.; Picot, D.; Jansonius, J. N.; Lesk, A. M.; Chothia, C. *J. Mol. Biol.* **1992**, *227*, 197.
(20) (a) Miertus, S.; Scrocco, E.; Tomasi, J. *Chem. Phys.* **1981**, *55*, 117. (b) Tomasi, J.; Persico, M. *Chem. Rev.* **1994**, *94*, 2027.
(21) (a) Amovilli, C.; Barone, V.; Cammi, R.; Cances, E.; Cossi, M.; Mennucci, B.; Pomelli, C. S.; Tomasi, J. *Adv. Quantum Chem.* **1998**, *32*, 227. (b) Barone, V.; Cossi, M. *J. Phys. Chem. A* **1998**, *102*, 1995. (c) Barone, V.; Cossi, M. *J. Chem. Phys.* **1998**, *109*, 6246.
(22) Arnaud, R.; Adamo, C.; Cossi, M.; Milet, A.; Vallee, Y.; Barone, V. *J. Am. Chem. Soc.* **2000**, *122*, 324.
(23) Cossi, M.; Barone, V. *J. Chem. Phys.* **2000**, *112*, 2427.
(24) Nielsen, P. A.; Norrby, P. O.; Liljefors, T.; Rega, N.; Barone, V. *J. Am. Chem. Soc.* **2000**, *122*, 3151.
(25) Adamo, C.; Barone, V. *Chem. Phys. Lett.* **2000**, *330*, 152. (b) Improta, R.; di Matteo, A.; Barone, V. *Theor. Chem. Acc.* **2000**, *104*, 273.
(26) Adamo, C.; Cossi, M.; Rega, N.; Barone, V. In *Theoretical Biochemistry. Processes and Properties of Biological Systems*; Eriksson, L. A., Ed.; Elsevier: New York, 2001; p 467.
(27) Ayala, P. Y.; Scuseria, G. E. *J. Comput. Chem.* **2000**, *21*, 1524.
(28) Elstner, M.; Jalkanen, K. J.; Knapp-Mohammady, M.; Frauenheim, Th.; Suhai, S. *Chem. Phys.* **2000**, *256*, 15.
(29) Varnek, A. A.; Glebov, A. S.; Feil, D. *J. Comput.Chem.* **1995**, *16*, 1.
(30) Rega, N.; Cossi, M.; Pomelli, C. S.; Tomasi, J. *Int. J. Quantum Chem.* **1999**, *73*, 219.
(31) Rega, N.; Scalmani, G.; Barone, V. Manuscript in preparation.
(32) Frisch, M. J.; Trucks, H. B.; Schegel, G. E.; Scuseria, M. A.; Robb, M. A.; Cheeseman, J. R.; Zakrzewski, V. G.; Montgomery, J. A. Jr.; Stratmann, R. E.; Burant, J. C.; Dapprich, S.; Millan, J. M.; Daniels, A. D.; Kudin, K. N.; Strain, M. C.; Farkas, O.; Tomasi, J.; Barone, V.; Cossi, M.; Cammi, R.; Menucci, B.; Pomellim, C.; Adamo, C.; Clifford, S.; Ochterskim, J.; Petersson, G. A.; Ayala, P. Y.; Cui, Q.; Morokuma, K.; Malick, D. K.; Rabuck, A. D.; Raghavachari, K.; Foresman, J. B.; Cioslowski, J.; Ortiz, J. V.; Stefanov, B. B.; Liu, G.; Liashenko, A.; Piskorz, P.; Komaromi, I.; Gomperts, R.; Martin, R. L.; Fox, F. D. J.; Keith, T.; Al-Laham, M. A.; Peng, C. Y.; Nanayakkara, A.; Gonzalez, C.; Challacombe, M.; Gill, P. M. W.; Johnson, B.; Chen, W.; Wong, M. W.; Andres, J. L.; Gonzalez, C.; Head-Gordon, M.; Replogle, E. S.; Pople, J. A. *Gaussian 99, Revision C.1*; Gaussian Inc.: Pittsburgh, PA, 2001.
(33) Rega, N.; Cossi, M.; Barone, V. *Chem. Phys. Lett.* **1998**, *293*, 221.
(34) Rega, N.; Cossi, M.; Barone, V. *J. Comput. Chem.* **1999**, *11*, 1186.
(35) Pomelli, C. S.; Tomasi, J.; Barone, V. *Theor. Chem. Acc.* **2001**, *105*, 446.
(36) Rega, N.; Cossi, M.; Scalmani, G.; Barone, V. Manuscript in preparation.
(37) Mayo, S. L.; Olafson, B. D.; Goddard, W. A., III. *J. Phys. Chem.* **1990**, *94*, 8897.
(38) Rappé, A. K.; Casewit, C. J.; Colwell, K. S.; Goddard, W. A., III; Skiff, W. M. *J. Am. Chem. Soc.* **1992**, *114*, 10024.
(39) Cornell, W. D.; Cieplak, P.; Bauly, C. I.; Gould, I. R.; Merz, K. M., Jr.; Ferguson, D. M.; Spellmeyer, D. C.; Fox, T.; Caldwell, J. W.; Kollman, P. A. *J. Am. Chem. Soc.* **1995**, *117*, 5179.
(40) Adamo, C.; Barone, V. *J. Chem. Phys.* **1999**, *110*, 6158.
(41) Hariharan, P. C.; Pople, J. A. *Theor. Chim. Acta* **1973**, *23*, 213.
(42) Gunnarson, O.; Lundqvist, B. I. *Phys. Rev. B* **1976**, *13*, 4274.
(43) Perdew, J. P.; Burke, K.; Ernzerhof, M. *Phys. Rev. Lett.* **1996**, *77*, 3685; **1997**, *78*, 1396 (Erratum).
(44) (a) Improta, R.; Barone, V.; Kudin, K.; Scuseria, G. E. *J. Chem. Phys.* **2001**, *114*, 2541. (b) Improta, R.; Benzi, C.; Barone, V. *J. Am. Chem. Soc.*, submitted.
(45) (a) Schlegel, H. B. *J. Comput. Chem.* **1982**, *3*, 214. (b) Farkas, O.; Schlegel, H. B. *J. Chem. Phys.* **1999**, *111*, 10806.
(46) Barone, V.; Cossi, M.; Tomasi, J. *J. Chem. Phys.* **1997**, *107*, 3210.
(47) Pascual-Ahuir, J. L.; Silla, E.; Tomasi, J.; Bonaccorsi, R. *J. Comput. Chem.* **1996**, *17*, 56.

(48) Pierotti, R. A. *Chem. Rev.* **1976**, *76*, 717.
(49) Floris, F. M.; Tomasi, J. *J. Comput. Chem.* **1986**, *10*, 616.
(50) Huyghues-Despointes, B. M. P.; Scholtz, J. M.; Baldwin, R. L. *Protein Sci.* **1993**, *2*, 1604.
(51) (a) Madison, V.; Kopple, K. D. *J. Am. Chem. Soc.* **1980**, *102*, 4855. (b) Beachy, M. D.; Chasman, D.; Murphy, R. B.; Halgren, T. A.; Friesner, R. A. *J. Am. Chem. Soc.* **1997**, *119*, 5908.
(52) Yoder, G.; Polese, A.; Silva, R. A. G. D.; Formaggio, F.; Crisma, M.; Broxterman, Q. B.; Kamphuis, J.; Toniolo, C.; Keiderling, T. A. *J. Am. Chem. Soc.* **1997**, *119*, 10278.
(53) Alemán, C.; Luque, F. J.; Orozco, M. *Chem. Phys.* **1994**, *189*, 573.

MA0106503